Microbiology (2009), **155**, 3860–3867 **DOI** 10.1099/mic.0.032854-0

Vesicle-associated melanization in *Cryptococcus neoformans*

Helene C. Eisenman,[1]†‡ Susana Frases,[1]†§ André M. Nicola,[1,2] Marcio L. Rodrigues[3] and Arturo Casadevall[1]

Correspondence
Arturo Casadevall
casadeva@aecom.yu.edu

[1]Department of Microbiology and Immunology, Albert Einstein College of Medicine, Bronx, New York 10461, USA

[2]Departamento de Biologia Celular, Universidade de Brasília, Brazil

[3]Laboratório de Estudos Integrados em Bioquímica Microbiana, Instituto de Microbiologia Professor Paulo de Góes, Universidade Federal do Rio de Janeiro, Rio de Janeiro 21941-590, Brazil

Received 16 July 2009
Revised 28 August 2009
Accepted 2 September 2009

Recently, several pathogenic fungi were shown to produce extracellular vesicles that contain various components associated with virulence. In the human pathogenic fungus *Cryptococcus neoformans*, these components included laccase, an enzyme that catalyses melanin synthesis. Spherical melanin granules have been observed in the cell wall of *C. neoformans*. Given that melanin granules have dimensions that are comparable to those of extracellular vesicles, and that metazoan organisms produce melanin in vesicular structures known as melanosomes, we investigated the role of vesicles in cryptococcal melanization. Extracellular vesicles melanized when incubated with the melanin precursor L-3,4-dihydroxyphenylalanine (L-DOPA). The kinetics of substrate incorporation into cells and vesicles was analysed using radiolabelled L-DOPA. The results indicated that substrate incorporation was different for cells and isolated vesicles. Acid-generated melanin ghosts stained with lipophilic dyes, implying the presence of associated lipid. A model for *C. neoformans* melanization is proposed that accounts for these observations and provides a mechanism for the assembly of melanin into relatively uniform spherical particles stacked in an orderly arrangement in the cell wall.

INTRODUCTION

Cryptococcus neoformans is a pathogenic yeast that is a significant health threat to persons with compromised immunity, such as patients with AIDS. Cryptococcosis is currently the fourth leading cause of death in Africa and it is estimated to affect one million individuals worldwide each year (Park *et al.*, 2009). *C. neoformans* is found in the environment, and serological studies have shown that infection is common even though disease is rare (Goldman *et al.*, 2001). Pulmonary infection rarely leads to disseminated disease, except in hosts with impaired immune systems. Alveolar macrophages are important in containing the infection, as is cell-mediated immunity (Eisenman *et al.*, 2007).

†These authors contributed equally to this work.

‡Present address: Department of Natural Sciences, Baruch College, 17 Lexington Avenue, New York, NY 10010, USA.

§Present Address: Laboratório de Biotecnologia (LABIO), Instituto Nacional de Metrologia, Normalização e Qualidade Industrial (INMETRO), Av. Nossa Senhora das Graças 50, Xerém, Rio de Janeiro 25 250 020, Brazil.

Abbreviations: DOPA, 3,4-dihydroxyphenylalanine; QELS, quasi-elastic light scattering; TEM, transmission electron microscopy.

The fungus has several traits that contribute to virulence. The major virulence factor is a polysaccharide capsule composed of glucuronoxylomannan, galactoxylomannan and mannoproteins (Janbon, 2004; McFadden *et al.*, 2006). In addition, *C. neoformans* secretes a number of enzymes that contribute to virulence, such as phospholipase B, urease and laccase. Other traits contributing to virulence are the ability to grow at 37 °C, and the ability to produce the pigment melanin (Casadevall *et al.*, 2003; Perfect, 2005). Melanin plays an important role in the virulence of fungi and their survival in the environment. In *C. neoformans*, melanin protects cells from phagocytosis by macrophages, a key step in the host defence against the yeast (Wang *et al.*, 1995). Melanization protects *C. neoformans* from UV irradiation, oxidative stress and extreme temperatures (Garcia-Rivera & Casadevall, 2001; Rosas & Casadevall, 1997; Wang & Casadevall, 1994). Melanization of *C. neoformans* depends on the presence of substrate, such as L-3,4-dihydroxyphenylalanine (L-DOPA) and other catecholamines (Garcia-Rivera *et al.*, 2005). In addition, it requires expression of laccase, a cell wall enzyme that is associated with virulence (Zhu *et al.*, 2001). In melanized cells, melanin is found in the cell wall of the yeast (Nosanchuk & Casadevall, 2003). Melanization of *C.*

neoformans cells is associated with acquired resistance to polyene- and echinocandin-class drugs and may be responsible for the refractoriness to therapy (Nosanchuk & Casadevall, 2006).

Recently, it was reported that vesicles found in the cell wall of *C. neoformans* are also secreted into the culture medium (Casadevall *et al.*, 2009; Rodrigues *et al.*, 2007). These vesicles contain lipids that are also present in the membranes of *C. neoformans*, such as glucosylceramide and the sterols ergosterol and obtusifoliol (Rodrigues *et al.*, 2007). Besides lipids, the vesicular contents include the capsular polysaccharide glucuronoxylomannan (Rodrigues *et al.*, 2007) and a variety of enzymes associated with virulence, such as laccase, urease and phosphatase (Rodrigues *et al.*, 2008). Thus, these vesicles may be involved in transport of virulence factors out of the cell. Indeed, extracellular vesicle secretion has been associated with cryptococcal virulence in an animal model of infection (Panepinto *et al.*, 2009).

Cellular and mechanistic details of the process of melanization in *C. neoformans* remain poorly understood. For example, melanization in *C. neoformans* involves the deposition of small granules on the cell wall, raising the question of how the enzymic reaction catalysed by laccase can produce the formation of relatively uniform spherical particles that are then assembled in the cell wall in concentric layers (Eisenman *et al.*, 2005). Another unanswered question is the mechanism by which cryptococcal cells avoid the toxicity of melanin precursors, a problem solved in mammalian cells by confining melanization to melanosomes (Graham *et al.*, 1978; Pavel, 1993; Tolleson, 2005). The goal of this study was to gain insights into the details of melanization of *C. neoformans* by investigating the relationship between vesicular transport and melanization. The cryptococcal vesicles were studied using physical and microscopic techniques. Since laccase activity was previously associated with vesicles, the kinetics of melanin substrate incorporation by cells and vesicles were investigated. Based on these data and information from previous studies, a model of vesicle-associated melanization in *C. neoformans* is proposed.

METHODS

***C. neoformans* strains.** The following strains were used: ATCC 24067 (serotype D; American Type Culture Collection) and H99 (serotype A, clinical isolate). Strain QGC8 contains complete deletions of the *LAC1* and *LAC2* genes. H99 is the wild-type parent strain for this laccase mutant (Pukkila-Worley *et al.*, 2005).

Isolation of vesicles. *C. neoformans* cells were inoculated into 1000 ml Erlenmeyer flasks containing 500 ml of a minimal medium composed of glucose (15 mM), $MgSO_4$ (10 mM), KH_2PO_4 (29.4 mM), glycine (13 mM), and thiamine.HCl (3 μM). Cells were incubated for 3 days at 30 °C with shaking. Vesicle isolation was performed according to a previously described protocol (Rodrigues *et al.*, 2007). Briefly, cells were separated from culture supernatants by centrifugation at 4000 ***g*** for 15 min at 4 °C. The supernatants were collected and centrifuged at 15 000 ***g*** (4 °C) to remove debris. The pellets were discarded, and the resulting supernatant was concentrated approximately 20-fold using an Amicon (Millipore) ultrafiltration system (cutoff, 100 000 Da). To ensure the removal of cells and cell debris, the concentrated culture fluid was again centrifuged as described above and the resulting supernatant was then centrifuged at 100 000 ***g*** for 1 h at 4 °C. The supernatants were discarded and the pellets suspended in 3 ml PBS and centrifuged at 100 000 ***g*** for 1 h at 4 °C.

Melanization of vesicles and liposomes. Isolated vesicles were incubated overnight at room temperature and at 4 °C in PBS with 1 mM L-DOPA (Sigma). For non-melanized controls in sizing experiments, vesicles were incubated without L-DOPA. Liposomes composed of phosphatidylcholine and ergosterol were obtained from Encapsula Nano Sciences. Liposomes (50 μl of a 20 mg ml^{-1} suspension) were suspended in a total volume of 500 μl PBS. L-DOPA was added to a final concentration of 1 mM. The liposomes were incubated overnight at room temperature.

Electron microscopy. Liposomes or vesicles (with or without L-DOPA) isolated from culture supernatants of *C. neoformans* by ultracentrifugation were fixed in 2.5 % (v/v) glutaraldehyde in 0.1 M cacodylate at room temperature for 2 h and then incubated overnight in 4 % (v/v) formaldehyde, 1 % (v/v) glutaraldehyde, 0.1 % (v/v) PBS. The vesicle samples were incubated for 90 min in 2 % (w/v) osmium tetroxide, serially dehydrated in ethanol, and embedded in Spurr's epoxy resin. Thin sections were obtained on a Reichert Ultracut and stained with 0.5 % (w/v) uranyl acetate and 0.5 % (w/v) lead citrate. Samples were observed in a JEOL 1200EX transmission electron microscope operating at 80 kV. To determine the size of the vesicles, photographs of the images were scanned and analysed in Adobe Photoshop. The line tool was used to measure across the width of the melanin layer, and the size was calculated based on magnification of the photograph. For negative-stain electron microscopy, purified vesicles were transferred to carbon- and Formvar-coated grids and negatively stained with 1 % phosphotungstic acid. The grids were then blotted dry before immediately observing in a JEOL 100CX II transmission electron microscope at 80 kV. The diameter of 1000 vesicles from 10 different fields was measured.

Measurement of vesicle size by quasi-elastic light scattering (QELS). Effective diameter and size distribution of melanized and non-melanized vesicles suspended in PBS were measured in a 90Plus/BI-MAS Multi Angle Particle Sizing analyser (Brookhaven Instruments). Vesicles in a liquid phase undergo Brownian motion that produces light scattering fluctuations that provide information on the size and heterogeneity of the sample. Laser illumination with monochromatic light results in a fluctuating signal, originating from the random motion of these vesicles; this was analysed by the autocorrelation function $C(t)$: $C(t)=Ae^{2\Gamma t}+B$. In this equation, t is the time delay, A and B are optical constants determined by the instrument design, and Γ is related to the relaxation of the fluctuations by $\Gamma=Dq^2$. The parameter q is calculated from the scattering angle θ, the laser light wavelength λ_0, and the refractive index (n) of the solvent from the equation $q=(2\pi n/\lambda_0)2sin(\theta/2)$. D was calculated from the equation $D=(K_BT)/(3\pi\eta(t)d)$, which assumes a spherical shape for the scattering particle, where K_B is Boltzmann's constant (1.38054×10^{-23} J deg^{-1}), T is the temperature in K (303 K), $\eta(t)$ is the viscosity of the liquid in which the particles are moving, and d is the particle diameter.

L-[^{14}C]DOPA incorporation analysis. *C. neoformans* cells (strains H99 and QGC8) were grown in chemically defined minimal medium for 2 days at 30 °C, 150 r.p.m., to a density of approximately 5×10^7 c.f.u. ml^{-1}. Cells were pelleted by centrifugation at 2000 r.p.m., 22 °C, for 10 min. Pellets were washed once with starvation medium

(0.2 g K_2HPO_4 l^{-1}, 0.1 g KH_2PO_4 l^{-1}), suspended in starvation medium and incubated overnight at 30 °C and 150 r.p.m. Cells were then collected by centrifugation again and suspended in starvation medium to a density of $1–2\times10^8$ c.f.u. ml^{-1}. As a control for incorporation studies, H99 cells were heat-killed at 65 °C for 1 h. Cells were plated on Sabouraud medium for c.f.u. determination. Cell suspensions (4 ml) were incubated with 4 μCi of a 54 mCi (1998 MBq) $mmol^{-1}$ solution of L-3,4-dihydroxyphenyl-[3-^{14}C]alanine (GE Healthcare) at 30 °C, 150 r.p.m. The final concentration of L-DOPA was approximately 0.005 mM. For comparison, dopamine concentrations in certain areas of the brain are approximately 0.06 mM (Felice *et al.*, 1978). Aliquots (250 μl) were removed at the indicated times over a 24 h time period and briefly centrifuged to pellet cells. The pellets were washed twice with 250 μl PBS to remove unincorporated label. Pellets were suspended in 250 μl PBS. L-[^{14}C]DOPA incorporation by vesicles and liposomes was performed similarly. Vesicles were prepared as described above and suspended in PBS. Liposomes (100 μl of a 20 mg ml^{-1} suspension) were suspended in PBS. L-[^{14}C]DOPA (1 μCi; 37 kBq) was added to 1 ml of vesicle or liposome suspension with *N*-(phosphonomethyl)glycine (Sigma) at the indicated concentrations and the mixture was incubated at either 4 °C or room temperature. The final concentration of L-DOPA was approximately 0.02 mM. At the indicated times, an aliquot (250 μl) was removed for counting. Samples were centrifuged at 100 000 ***g***, 4 °C, for 1 h in a TLA 100.3 rotor (Beckman). Pellets were washed once with 250 μl PBS. Total c.p.m. in the supernatants and pellets were determined by liquid scintillation counting in an LKB Wallac 1217 Rackbeta liquid scintillation counter. The percentage incorporation was calculated from $c.p.m._{pellet}/(c.p.m._{pellet}+c.p.m._{supernatant})$. To control for solubility of L-DOPA in lipids, L-[^{14}C]DOPA (0.25 μCi; 9.25 kBq) was added to PBS (0.5 ml). The solution was extracted with olive oil or mineral oil (0.5 ml). The aqueous and lipid phases were analysed by liquid scintillation counting.

Fluorescence microscopy with lipophilic probes. The lipophilic probe Vybrant DiI (Invitrogen), a solution of 1,1′-dioctadecyl-3,3,3′,3′-tetramethylindocarbocyanine perchlorate, was used to stain melanin ghosts, which were prepared as described before (Rosas *et al.*, 2000). Briefly, cells were incubated with lysing enzymes, chemically denatured with guanidine thiocyanate, subjected to proteolysis, extracted with chloroform, and boiled in hydrochloric acid. The resulting particles, or melanin 'ghosts', were dialysed against water for 10 days. An aliquot that was not extracted with chloroform was also prepared. Both melanin samples were then stained for 1 h with 5 μM DiI. The ghosts were then suspended in mounting medium (0.1 M propylgallate in 1 : 1 glycerol/PBS) and imaged on an Olympus AX70 microscope using a 100× objective.

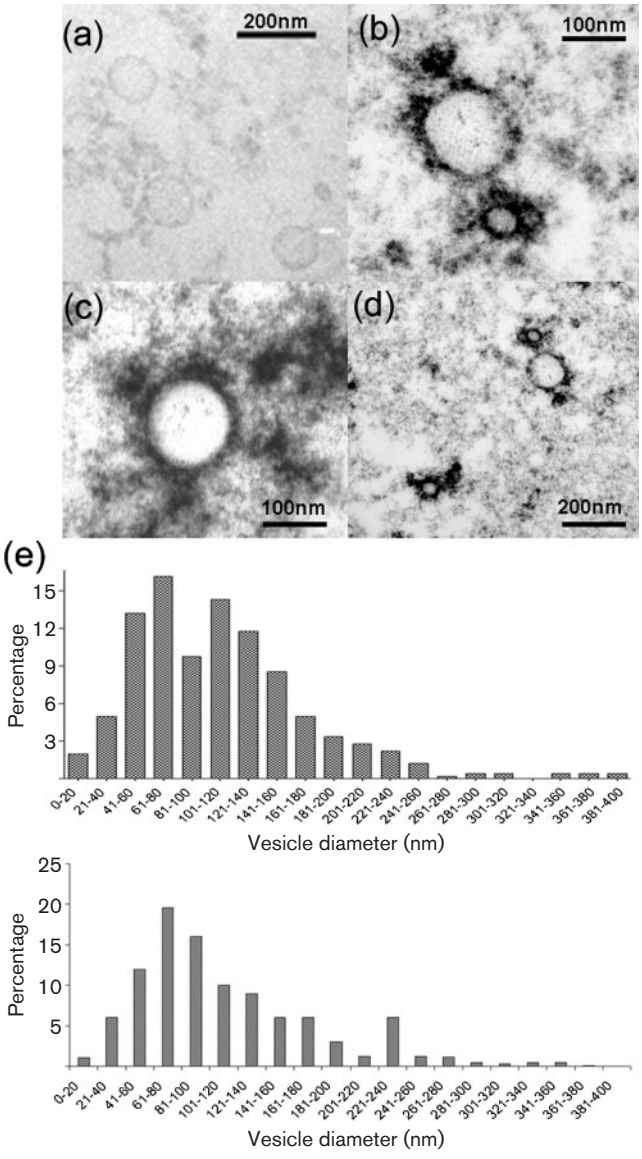

Fig. 1. Size distribution of cryptococcal vesicles studied by TEM. (a) Non-melanized vesicles. (b–d) Different sizes of melanized vesicles. (e) Size distribution of non-melanized (top) and melanized (bottom) vesicles as determined by TEM.

RESULTS

Structural analysis of vesicle melanization

To determine whether vesicles are involved in melanization of *C. neoformans*, we studied the ability of isolated vesicles to melanize by analysing the structure of vesicles incubated with melanization substrate. Vesicles isolated from *C. neoformans* culture supernatant were able to melanize after incubation with L-DOPA, as indicated by darkly stained material around the vesicle when visualized by transmission electron microscopy (TEM) (Fig. 1a–d). Three different methods were used to evaluate the size distribution of vesicles: two electron microscopy techniques and dynamic light scattering analysis (QELS) of vesicle suspensions. Determination of the diameter of melanized and non-melanized vesicles by TEM showed that the most common diameter of non-melanized vesicles was between 60 and 160 nm. The mean size of non-melanized vesicles was 112 nm (standard error, 3.189) and the mean size of melanized vesicles was 114 nm (standard error, 2.897) (Fig. 1e). TEM is optimal for providing ultrastructural details but has the drawback that sectioning can occur anywhere in the vesicular sphere, such that the mean diameter for a vesicle population measured by TEM is likely to be lower than the true equatorial diameter. Therefore QELS was performed to measure vesicle size.

Values of effective vesicle diameter obtained by QELS were significantly larger than those determined by TEM ($P<0.05$). Most vesicles were in the 160–260 nm range, with an additional smaller population of diameter 20–40 nm (Fig. 2c, d). Furthermore, the QELS results showed different size distributions for melanized and non-melanized vesicles. Melanized vesicles showed an effective diameter between 321 and 380 nm, whereas non-melanized vesicles had a diameter of 160–260 nm (Fig. 2c, d).

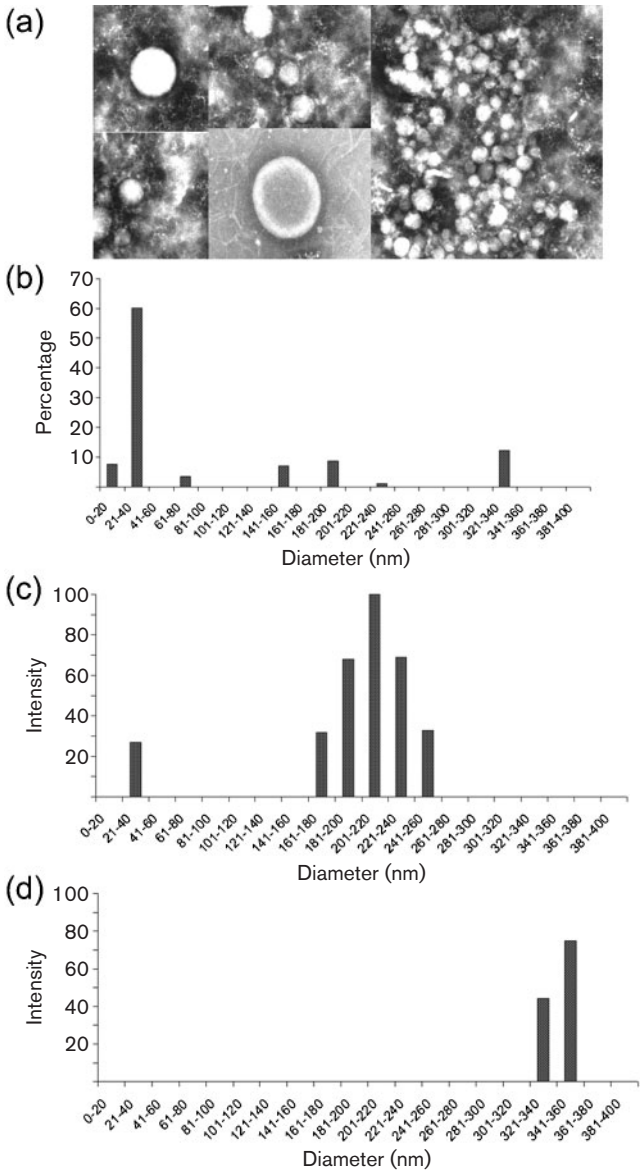

Fig. 2. (a) Composite panel of representative electron micrographs of negatively stained melanized vesicles. (b) Size distribution of *C. neoformans* vesicles as determined by electron microscopy with negative staining. (c, d) Size distribution of non-melanized (c) and melanized (d) vesicles as determined by QELS.

Electron microscopy with negative staining revealed a smaller population of vesicles with diameters in the 21–40 nm range (Fig. 2a, b). Whether this represents an enrichment of the small vesicles through the negative staining protocol or vesicle shrinkage is unclear. The fact that QELS also showed a population of smaller vesicles suggests that the vesicles are heterogeneous in size.

Microscopic analysis of lipid association with melanin

If melanization occurs in vesicles, we reasoned that lipid may be associated with melanin due to the proximity of lipid membranes to the site of melanin polymerization. Purified *C. neoformans* melanin ghosts were stained with the lipophilic probe DiI, which was used to stain *C. neoformans* extracellular vesicles (Nicola *et al.*, 2009). Since the melanin purification protocol includes two extractions with chloroform, we also stained a different aliquot of the same melanin preparation that had not been subjected to the extraction steps. Ghosts that were not extracted with chloroform bound more DiI than the ones that did, suggesting that some lipid is associated with purified melanin (Fig. 3).

Incorporation of melanization substrate by *C. neoformans*

The kinetics of substrate incorporation into melanin was studied by measuring the incorporation of L-[^{14}C]DOPA into cells and vesicles. First, incorporation of L-[^{14}C]DOPA by *C. neoformans* cells of wild-type (H99), laccase deletion mutant (QGC8) and heat-killed wild-type was analysed.

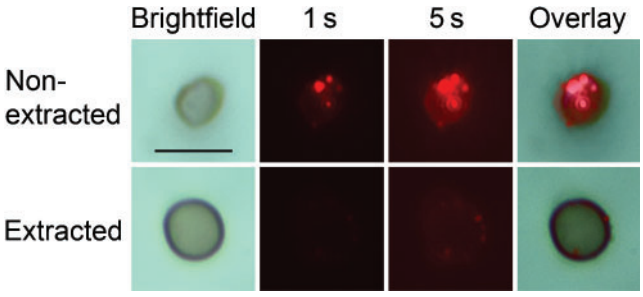

Fig. 3. DiI staining of *C. neoformans* melanin ghosts. Melanin ghosts that were, or were not, subjected to a double extraction with chloroform were stained with DiI and imaged by epifluorescence microscopy. Exposure time and filter sets were maintained constant for both samples. The melanin ghosts are thoroughly but dimly labelled and contain a few brighter spots. The two images shown are representative of the pattern we observed of less intense fluorescence in the ghosts that were subjected to chloroform extraction. Scale bar, 5 μm. Note that the size of spots from DiI staining is altered by the process of light collection and consequently no inferences as to the size of the spots should be made from the images shown.

Cells were incubated with the L-[^{14}C]DOPA and the percentage of label incorporation by the cells was monitored by liquid scintillation counting (Fig. 4a). Initially, the percentage incorporation for all samples was very low. Over time, the live wild-type strain accumulated L-DOPA. Ninety-four per cent of the label was found in the cell pellets of these strains by 24 h. In contrast, the heat-killed and laccase-deficient cells accumulated less radioactive label. At 24 h, 36 % of the label was found in the cell pellets for the laccase-deficient samples, significantly less than for wild-type cells ($P<0.05$). The label associated with cells of the laccase deletion strain could be due to autopolymerization of the L-DOPA, formation of L-DOPA adducts, or uptake of the L-DOPA into the cells without incorporation into melanin.

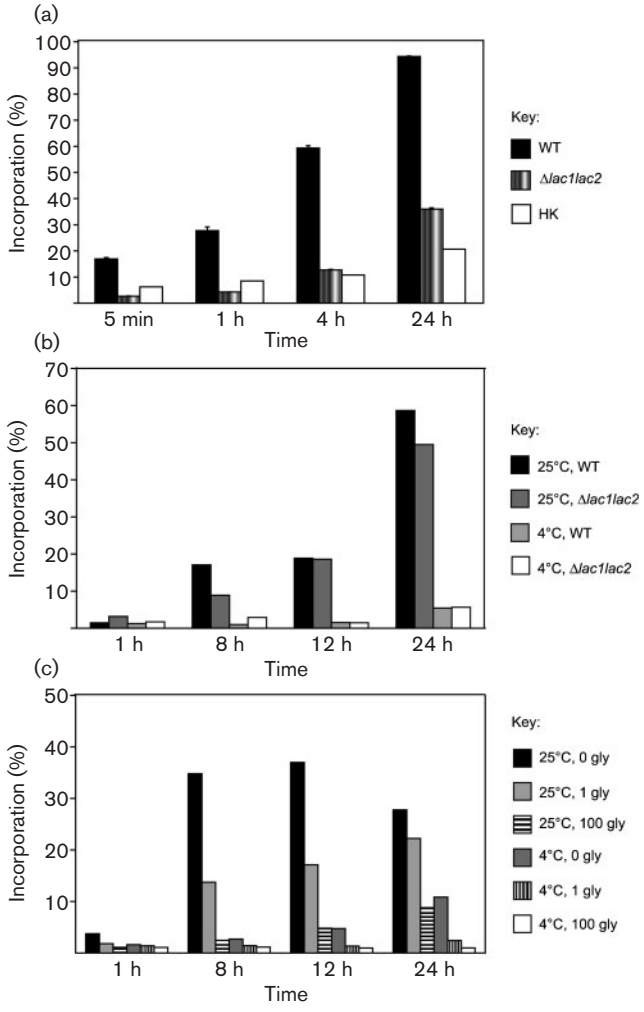

Fig. 4. L-DOPA incorporation kinetics. Cells were incubated with L-[^{14}C]DOPA. At the indicated times, aliquots were removed and centrifuged to separate the cells from the supernatant. Percentage incorporation was calculated from the counts in the cell pellet divided by total counts. (a) Incorporation results for cells of the strains H99 (wild-type, WT) and QGC8 (Δ*lac1lac2*), and heat-killed H99 (HK). (b) Incorporation results for vesicles isolated from H99 (WT) and QGC8 (Δ*lac1lac2*) (c) Incorporation results for liposomes. The experiment was performed with or without glyphosate (gly) at 1 or 100 μg ml^{-1}.

We hypothesized that a similar pattern of L-DOPA incorporation would be observed with purified extracellular vesicles. To confirm this, vesicles were prepared from both wild-type and laccase deletion strains and incubated with L-[^{14}C]DOPA over a 24 h time period. In contrast to our hypothesis, vesicles derived from culture supernatants of both wild-type and laccase mutant *C. neoformans* incorporated label to similar maximum levels (59 % and 49 %, respectively) (Fig. 4b). Thus, the pattern observed for vesicles was different from that for cells, suggesting a laccase-independent mechanism for incorporation of L-DOPA. This uptake was not due simply to solubility of L-DOPA in lipid, since L-[^{14}C]DOPA was not extractable by oils (data not shown). To determine if L-DOPA polymerization was induced simply by the presence of lipid bilayers, L-[^{14}C]DOPA was incubated with liposomes composed of phosphatidylcholine and ergosterol, approximating fungal membranes. The liposomes accumulated L-[^{14}C]DOPA to a maximum level of 37 % (Fig. 4c). The accumulation of L-[^{14}C]DOPA was equally inhibited by lower temperature in both laccase-positive and laccase-negative vesicles, as well as in liposomes. Accumulation in liposomes was also inhibited by glyphosate, an inhibitor of L-DOPA polymerization (Nosanchuk *et al.*, 2001). Liposomes incubated overnight with L-DOPA turned black (data not shown). However, when viewed by TEM, there were no detectable differences between liposomes incubated with or without L-DOPA (Fig. 5), suggesting that the accumulation of radiolabelled L-DOPA in liposomes was not due to melanization, but rather to autopolymerization of L-DOPA.

DISCUSSION

In this study we examined the potential role of vesicles in melanization of *C. neoformans*, a process that is important for both virulence and survival of the fungus. Previous studies suggested that melanization occurred when laccase in the cell wall oxidized a substrate, such as L-DOPA, ultimately resulting in polymerization of melanin (Waterman *et al.*, 2007; Zhu *et al.*, 2001). However, recent studies showing the presence of cell-wall-associated vesicles exhibiting laccase activity raised the possibility of the involvement of vesicles in melanization (Rodrigues *et al.*, 2008).

Our first attempt to link vesicles and melanization was to measure the size of the vesicles. Three methods were used to study vesicle size and heterogeneity: two electron microscopic techniques and a light-scattering method (QELS). Each method produced a different size distribution but, reassuringly, there was some overlap in the results with all three techniques. Negative staining revealed a much higher proportion of a smaller vesicle population

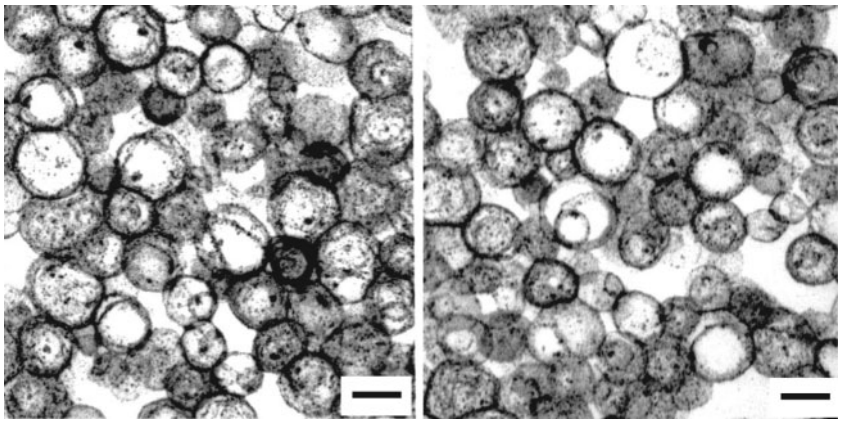

Fig. 5. TEM of liposomes incubated overnight with (left) or without (right) 1 mM L-DOPA. Scale bars, 100 nm.

that may represent vesicle shrinkage. Alternatively, the smaller vesicles observed with QELS may be preferentially deposited on the grids used for electron microscopy. All three techniques indicated considerable heterogeneity in vesicle diameter, but revealed a population of vesicles with diameters that are similar to melanin granules.

The variability in the vesicle population measured by the various techniques may be real and/or may reflect some of the limitations of the techniques used. Some of the size fluctuation may be due to sample preparation, particularly fusion of hydrophobic membranes during centrifugation to produce larger vesicles, or aggregation of particles. TEM size determinations are likely to be underestimated somewhat because 2D information is being used to generate 3D diameter. Kong *et al.* (2005) proposed a correction factor of 1.27 for such measurements. With this correction, the mean diameter by TEM is 142 nm, which is still less than that determined by QELS. However, a comparative study of sizing techniques for the study of liposomes showed that QELS probably overestimates sizes because smaller particles are less likely to be detected by this method (Egelhaaf *et al.*, 1996). Overall, the results suggest that there are at least two different size populations of vesicles: small vesicles in the range 20–40 nm that were detected by both negative staining and QELS, and a larger population in the range 140–260 nm that seemed to increase in size upon melanization.

To test the hypothesis that vesicles are involved in melanization, we investigated the ability of isolated vesicles to melanize. When vesicles were incubated with L-DOPA, an electron-dense material could be seen outside the vesicles by electron microscopy. This material was not observed when liposomes, which do not contain laccase, were incubated with L-DOPA. When the size of L-DOPA-melanized vesicles was analysed, they were found by QELS to be larger than non-melanized vesicles. This is consistent with melanin polymerizing on the vesicle surface and increasing its apparent diameter, and/or aggregation of melanized vesicles. We suspect that this process is different from that which produces spherical melanin particles in the cell wall and could reflect the fact that the vesicles studied were obtained from the supernatant and may have been designed for export rather than cell wall melanization.

Melanization of vesicles was further studied by determining the kinetics of incorporation of a radiolabelled melanin substrate, L-[^{14}C]DOPA. Surprisingly, both wild-type and laccase mutant vesicles accumulated radiolabelled L-DOPA with similar kinetics. To test if this was due to the lipid, or if protein components of vesicles were required for uptake, the experiment was repeated using liposomes. The liposomes also incorporated the labelled L-DOPA. Given that L-DOPA slowly autopolymerizes to melanin we surmise that lipid surfaces may catalyse this process. This would suggest that, in *C. neoformans* cells, mechanisms exist to prevent L-DOPA autopolymerization in the absence of laccase, since cells of the laccase deletion strain incorporated little of the labelled substrate compared to wild-type cells.

Based on these data we propose a model for melanization in which melanin synthesis occurs in vesicles. This model is attractive because it explains several observations. First, it suggests an explanation for the fact that melanin particles are roughly spherical and of a relatively uniform size (Eisenman *et al.*, 2005) that closely approximates that of vesicles. In this regard, melanization in a vesicle solves the problem of accounting for how a free-radical reaction produces a spherical particle. Second, the melanization-within-lipid vesicle model also suggests an explanation for the observation that melanin in the cell wall is assembled in concentric layers (Eisenman *et al.*, 2005). Such a regular arrangement could be achieved by ordering laccase-containing vesicles in the cell wall. Third, the melanization-within-vesicles hypothesis suggests an explanation for the NMR observation that aliphatic compounds are associated with melanin (Zhong *et al.*, 2008) and for the observation in this study of lipid associated with melanin 'ghosts'. Localization of melanin synthesis to vesicles would obviate the problem of explaining how the cell avoids toxicity from the highly reactive intermediates generated by oxidation of L-DOPA. Furthermore, this model provides a way to interpret the very interesting finding that *C. neoformans* chitin synthase mutants exhibited a melanization phenotype whereby the pigment was released to the

extracellular space and diffused into the agar (Banks *et al.*, 2005; Baker *et al.*, 2007). We suggest that this phenotype could result if laccase-containing vesicles could not be retained by the chitin-defective cell wall (Banks *et al.*, 2005). Lastly, this hypothesis suggests a mechanism by which melanized cell walls could be rapidly remodelled by the reshuffling of melanized vesicles, given that there are no differences in replication rate of melanized and non-melanized cells (Nosanchuk & Casadevall, 2003).

The melanization-in-vesicle model would also suggest a mechanism for the problem of cell budding through a melanized cell wall. Scanning electron microscopy of melanin 'ghosts' has shown melanized bud scars with a different granularity in melanin particle distribution. Given the resistance of melanin to enzymic and acid digestion it is difficult to conceive of mechanisms by which a replicating cell could rapidly open a budding pore for the emergence of a nascent cell and then reseal it. However, this problem is obviated if the mother cell only has to rearrange vesicles containing melanin by altering the cell wall components that hold such structures in place. Despite its attractive qualities we are fully cognisant that major facets of the model need to be experimentally established. We nevertheless hope that in proposing such a model we will encourage experiments to validate or refute it.

Recent work on vesicles in *C. neoformans* has suggested that these structures may contribute to pathogenesis by transporting virulence factors, including enzymes, out of the fungal cell (Casadevall *et al.*, 2009; Rodrigues *et al.*, 2008). The current study suggests that vesicles could also play a role in melanization. The existence of fungal melanosomes has been suggested for *Fonsecaea pedrosoi*, where electron microscopy has also shown electron-dense cytoplasmic structures in melanized cells (Franzen *et al.*, 2008). Localization of melanin synthesis to either intracellular vesicles that are subsequently transferred to cell wall and/or laccase-containing vesicles in the cell wall provides a fungal parallel to mammalian melanosomes, which are also synthesized inside melanocytes and exported to keratinocytes. Given that animals and fungi are closely related kingdoms the idea that both groups of eukaryotes solved the problem of melanin synthesis by confining melanization to lipid vesicles is intellectually appealing.

ACKNOWLEDGEMENTS

A. C. was supported by NIH grants AI33774, HL59842, AI33142 and AI52733. M. L. R. is supported by grants from the Brazilian agencies FAPERJ and CNPq. In addition, we thank the Analytical Imaging Facility at Albert Einstein College of Medicine for their assistance with the electron microscopy experiments.

REFERENCES

Baker, L. G., Specht, C. A., Donlin, M. J. & Lodge, J. K. (2007). Chitosan, the deacetylated form of chitin, is necessary for cell wall integrity in *Cryptococcus neoformans*. *Eukaryot Cell* **6**, 855–867.

Banks, I. R., Specht, C. A., Donlin, M. J., Gerik, K. J., Levitz, S. M. & Lodge, J. K. (2005). A chitin synthase and its regulator protein are critical for chitosan production and growth of the fungal pathogen *Cryptococcus neoformans*. *Eukaryot Cell* **4**, 1902–1912.

Casadevall, A., Steenbergen, J. N. & Nosanchuk, J. D. (2003). 'Ready made' virulence and 'dual use' virulence factors in pathogenic environmental fungi – the *Cryptococcus neoformans* paradigm. *Curr Opin Microbiol* **6**, 332–337.

Casadevall, A., Nosanchuk, J. D., Williamson, P. & Rodrigues, M. L. (2009). Vesicular transport across the fungal cell wall. *Trends Microbiol* **17**, 158–162.

Egelhaaf, S. U., Wehrli, E., Müller, M., Adrian, M. & Schurtenberger, P. (1996). Determination of the size distribution of lecithin liposomes: a comparative study using freeze fracture, cryoelectron microscopy, and dynamic light scattering. *J Microsc* **184**, 214–228.

Eisenman, H. C., Nosanchuk, J. D., Webber, J. B., Emerson, R. J., Camesano, T. A. & Casadevall, A. (2005). Microstructure of cell wall-associated melanin in the human pathogenic fungus *Cryptococcus neoformans*. *Biochemistry* **44**, 3683–3693.

Eisenman, H. C., Casadevall, A. & McClelland, E. E. (2007). New insights on the pathogenesis of invasive *Cryptococcus neoformans* infection. *Curr Infect Dis Rep* **9**, 457–464.

Felice, L. J., Felice, J. D. & Kissinger, P. T. (1978). Determination of catecholamines in rat brain parts by reverse-phase ion-pair liquid chromatography. *J Neurochem* **31**, 1461–1465.

Franzen, A. J., Cunha, M. M., Miranda, K., Hentschel, J., Plattner, H., da Silva, M. B., Salgado, C. G., de Souza, W. & Rozental, S. (2008). Ultrastructural characterization of melanosomes of the human pathogenic fungus *Fonsecaea pedrosoi*. *J Struct Biol* **162**, 75–84.

Garcia-Rivera, J. & Casadevall, A. (2001). Melanization of *Cryptococcus neoformans* reduces its susceptibility to the antimicrobial effects of silver nitrate. *Med Mycol* **39**, 353–357.

Garcia-Rivera, J., Eisenman, H. C., Nosanchuk, J. D., Aisen, P., Zaragoza, O., Moadel, T., Dadachova, E. & Casadevall, A. (2005). Comparative analysis of *Cryptococcus neoformans* acid-resistant particles generated from pigmented cells grown in different laccase substrates. *Fungal Genet Biol* **42**, 989–998.

Goldman, D. L., Khine, H., Abadi, J., Lindenberg, D. J., Pirofski, L., Niang, R. & Casadevall, A. (2001). Serologic evidence for *Cryptococcus neoformans* infection in early childhood. *Pediatrics* **107**, E66.

Graham, D. G., Tiffany, S. M. & Vogel, F. S. (1978). The toxicity of melanin precursors. *J Invest Dermatol* **70**, 113–116.

Janbon, G. (2004). *Cryptococcus neoformans* capsule biosynthesis and regulation. *FEMS Yeast Res* **4**, 765–771.

Kong, M., Bhattacharya, R., James, C. & Basu, A. (2005). A statistical approach to estimate the 3D size distribution of spheres from 2D size distributions. *Geol Soc Am Bull* **117**, 244–249.

McFadden, D., Zaragoza, O. & Casadevall, A. (2006). The capsular dynamics of *Cryptococcus neoformans*. *Trends Microbiol* **14**, 497–505.

Nicola, A. M., Frases, S. & Casadevall, A. (2009). Lipophilic dye staining of *Cryptococcus neoformans* extracellular vesicles and capsule. *Eukaryot Cell* **8**, 1373–1380.

Nosanchuk, J. D. & Casadevall, A. (2003). Budding of melanized *Cryptococcus neoformans* in the presence or absence of L-dopa. *Microbiology* **149**, 1945–1951.

Nosanchuk, J. D. & Casadevall, A. (2006). Impact of melanin on microbial virulence and clinical resistance to antimicrobial compounds. *Antimicrob Agents Chemother* **50**, 3519–3528.

Nosanchuk, J. D., Ovalle, R. & Casadevall, A. (2001). Glyphosate inhibits melanization of *Cryptococcus neoformans* and prolongs survival of mice after systemic infection. *J Infect Dis* **183**, 1093–1099.

Panepinto, J., Komperda, K., Frases, S., Park, Y. D., Djordjevic, J. T., Casadevall, A. & Williamson, P. R. (2009). Sec6-dependent sorting of fungal extracellular exosomes and laccase of *Cryptococcus neoformans*. *Mol Microbiol* **71**, 1165–1176.

Park, B. J., Wannemuehler, K. A., Marston, B. J., Govender, N., Pappas, P. G. & Chiller, T. M. (2009). Estimation of the current global burden of cryptococcal meningitis among persons living with HIV/AIDS. *AIDS* **23**, 525–530.

Pavel, S. (1993). Dynamics of melanogenesis intermediates. *J Invest Dermatol* **100**, 162S–165S.

Perfect, J. R. (2005). *Cryptococcus neoformans*: a sugar-coated killer with designer genes. *FEMS Immunol Med Microbiol* **45**, 395–404.

Pukkila-Worley, R., Gerrald, Q. D., Kraus, P. R., Boily, M. J., Davis, M. J., Giles, S. S., Cox, G. M., Heitman, J. & Alspaugh, J. A. (2005). Transcriptional network of multiple capsule and melanin genes governed by the *Cryptococcus neoformans* cyclic AMP cascade. *Eukaryot Cell* **4**, 190–201.

Rodrigues, M. L., Nimrichter, L., Oliveira, D. L., Frases, S., Miranda, K., Zaragoza, O., Alvarez, M., Nakouzi, A., Feldmesser, M. & Casadevall, A. (2007). Vesicular polysaccharide export in *Cryptococcus neoformans* is a eukaryotic solution to the problem of fungal trans-cell wall transport. *Eukaryot Cell* **6**, 48–59.

Rodrigues, M. L., Nakayasu, E. S., Oliveira, D. L., Nimrichter, L., Nosanchuk, J. D., Almeida, I. C. & Casadevall, A. (2008). Extracellular vesicles produced by *Cryptococcus neoformans* contain protein components associated with virulence. *Eukaryot Cell* **7**, 58–67.

Rosas, A. L. & Casadevall, A. (1997). Melanization affects susceptibility of *Cryptococcus neoformans* to heat and cold. *FEMS Microbiol Lett* **153**, 265–272.

Rosas, A. L., Nosanchuk, J. D., Gomez, B. L., Edens, W. A., Henson, J. M. & Casadevall, A. (2000). Isolation and serological analyses of fungal melanins. *J Immunol Methods* **244**, 69–80.

Tolleson, W. H. (2005). Human melanocyte biology, toxicology, and pathology. *J Environ Sci Health C Environ Carcinog Ecotoxicol Rev* **23**, 105–161.

Wang, Y. & Casadevall, A. (1994). Decreased susceptibility of melanized *Cryptococcus neoformans* to UV light. *Appl Environ Microbiol* **60**, 3864–3866.

Wang, Y., Aisen, P. & Casadevall, A. (1995). *Cryptococcus neoformans* melanin and virulence: mechanism of action. *Infect Immun* **63**, 3131–3136.

Waterman, S. R., Hacham, M., Panepinto, J., Hu, G., Shin, S. & Williamson, P. R. (2007). Cell wall targeting of laccase of *Cryptococcus neoformans* during infection of mice. *Infect Immun* **75**, 714–722.

Zhong, J., Frases, S., Wang, H., Casadevall, A. & Stark, R. E. (2008). Following fungal melanin biosynthesis with solid-state NMR: biopolymer molecular structures and possible connections to cell-wall polysaccharides. *Biochemistry* **47**, 4701–4710.

Zhu, X., Gibbons, J., Garcia-Rivera, J., Casadevall, A. & Williamson, P. R. (2001). Laccase of *Cryptococcus neoformans* is a cell wall-associated virulence factor. *Infect Immun* **69**, 5589–5596.

Edited by: J. Pla